Available online at www.sciencedirect.com
ScienceDirect
Ceramics International 36 (2010) 1503–1509
CERAMICS INTERNATIONAL
www.elsevier.com/locate/ceramint

High internal phase emulsion as reaction medium for precipitating brushite crystals

H.N. Lim [a,*], A. Kassim [a], N.M. Huang [b], K.H. Lee [c], A. Syahida [c], C.H. Chia [d]

[a] Chemistry Department, Faculty of Science, Universiti Putra Malaysia, 43400 UPM Serdang, Selangor, Malaysia
[b] Solid State Physics Research Laboratory, Physics Department, Faculty of Science, University of Malaya, 50603 Kuala Lumpur, Malaysia
[c] Biochemistry Department, Faculty of Biotechnology and Biomolecular Sciences, Universiti Putra Malaysia, 43400 UPM Serdang, Selangor, Malaysia
[d] School of Applied Physics, Faculty of Science and Technology, Universiti Kebangsaan Malaysia, 43600 Bangi, Selangor Darul Ehsan, Malaysia

Received 1 June 2009; received in revised form 29 December 2009; accepted 2 February 2010
Available online 9 March 2010

Abstract

This present work was aimed at fabrication of brushite crystals using oil-in-water high internal phase emulsion as a reaction medium. The oil phase of more than 75 wt.% was dispersed in the continuous aqueous phase. Due to the high oil volume fraction, the oil droplets were no longer spherical but were squeezed to take the shape of polyhedral. The morphology of the crystals was influenced by the structure of the emulsion and precursor concentration. The crystals were subjected to cytotoxicity test to ensure their compatibility with synoviocytes, which are cells that line the knee joints of rabbits. The crystals were able to sustain the cells for 5 days, which manifest their potential as osteoconductive coatings.

Keywords: E. Biomedical applications; High internal phase emulsion; Brushite

1. Introduction

Chemical analysis shows the presence of calcium and phosphate as principal constituents of natural bone, enamel and dentin. Synthetic calcium phosphates could be fabricated similar to the crystallographic structure of natural bone, enamel and dentin [1]. Calcium phosphates have a wide range of applications in tissue engineering, treatment of bone diseases and controlled drug delivery systems [2]. They have excellent biocompatibility and bone bonding or bone regeneration properties. Moreover, they have the ability to enhance bone growth across a gap around an implant in both stable and unstable mechanical conditions and even convert motion-induced fibrous membrane into a bony anchorage [3].

Porous calcium phosphate ceramic coatings are often applied on strong and load-bearing core materials for biological fixation or osteointegration of load-bearing implants such as hip stems and dental roots. Porous materials are associated with the connective tissue of vertebrae, where they form the main part of the bone. Studies have indicated that pores of calcium phosphates are necessary for controlled bioactivity and bioresorbability [4,5]. Numerous studies have been carried out to investigate calcium phosphate coatings on metal and polymer implants. Calcium phosphates have been used as surface coatings on many types of bioinert metallic and ceramic substrates, such as titanium and alumina [6]. Taniguchi et al. [7] demonstrated that sintered calcium phosphates showed excellent biocompatibility with soft tissues such as skin, muscle and gum, and designed a percutaneous catheter surrounded by calcium phosphates to prevent bacterial infections.

In contact with biological fluids, calcium phosphate ceramics degrade via dissolution–reprecipitation mechanisms [8]. Under physiological conditions, this dissolution process is highly dependent on the nature of the calcium phosphate substrate and their thermodynamic stability, for example (in order of increasing solubility), hydroxyapatite (HA) < tricalcium phosphate (TCP) < octacalcium phosphate (OCP) < bicalcium phosphate dihydrate (DCPD) [9].

Brushite (DCPD) has attracted great interests amongst researchers as a resorbable bone replacement material due to its

* Corresponding author at: Chemistry Department, Faculty of Science, Universiti Putra Malaysia, 43400 UPM Serdang, Selangor, Malaysia.
Tel.: +60 16 3301609; fax: +60 35 8911088.
E-mail address: janet_limhn@yahoo.com (H.N. Lim).

0272-8842/$36.00
doi:10.1016/j.ceramint.2010.02.029

higher solubility at pH 7.4 in physiological conditions compared to other calcium phosphate crystalline phases [10,11]. The biocompatibility and degradation of brushite have been demonstrated in several in vitro and in vivo studies [12–14]. Therefore, brushite is a suitable candidate as a bioceramic coating in addition to the association with the osteoconductivity of calcium phosphates [15]. Moreover, a porous bioceramic external layer on a metallic or ceramic substrate, which is used as a bone implant, will promote bone ingrowth [16]. In treating bone diseases like osteoarthritis, cells could be loaded onto bioceramic-coated matrices before implanting the cell-loaded matrices into a host body for achieving bone tissue regeneration [17].

High internal phase emulsion (HIPE) is gaining considerable interests amongst researchers as a reaction medium for the preparation of meso/macroporous materials [18]. This particular emulsion consists of disperse phase which exceeds the close packing volume limit of 0.74, the point where the droplets just touch each other [19]. Emulsion droplets of sizes between 0.5 μm and 5.0 μm offer a reaction medium fit for the creation of micron-sized pores into an inorganic or organic matrix [2].

In this work, calcium phosphate crystals with unique morphologies were successfully synthesized through palm olein-in-water (O/W) HIPE. Cytotoxicity test was performed on the crystals using synovial intimal cells, termed synoviocytes [20], to investigate their compatibility with the continuous cell line from the periarticular soft tissue lining the knee joints of rabbits. The periarticular soft tissue is subjected to considerable experimental scrutiny owing to its involvement in bone diseases [21–25]. This tissue lining contains a surface layer, known as the synovium, which is 2–3 cells deep. The synovium is underlain by a connective tissue framework with varying amounts of fibrous, areolar and fatty tissues, which is supported by a thick, collagenous tissue called the ''capsule'' [26]. Studies indicate that synovial tissues are enriched with cells of the monocyte/macrophage lineage that, with appropriate stimuli, can be induced to differentiate into preosteoclasts and ultimately into fully functional osteoclasts [27–29]. In addition, several studies have shown that synovial tissues are a rich source of a number of cytokines and inflammatory mediators that possess the capacity to induce the recruitment, differentiation and activation of osteoclasts [30–36]. Designated HIG-82 line was produced by spontaneous establishment of an aging, late-passage culture of primary cells.

2. Experimental

2.1. Calcium phosphate fabrication

In order to fabricate calcium phosphate crystals through the HIPE processing route, two aqueous solutions containing (a) 5.0 wt.% Brij 35 (Fluka) and 0.50 M calcium chloride, $CaCl_2{\cdot}2H_2O$ (Sigma–Aldrich) and (b) 5.0 wt.% Brij 35 and 0.30 M disodium hydrogen phosphate, Na_2HPO_4 (Sigma–Aldrich) were prepared. Brij 35 is polyoxyethylene lauryl ether $(C_2H_4O)_{23}C_{12}H_{25}OH$ with CAS No. 9002-92-0. Refined–bleached–deodorized (RBD) palm olein (Moi Foods Malaysia Sdn. Bhd.) as oil phase was added drop wise into each of the aqueous phase equally while stirring. The oil volume fraction (Ø) was 0.80, which was calculated based on Eq. (1):

$$\varnothing = \frac{m_o/\rho_o}{(m_o/\rho_o) + (m_w/\rho_w)} \quad (1)$$

where m_o/ρ_o is the volume of oil and m_w/ρ_w is the volume of water [37].

The mixtures were then mixed and homogenized at 1500 rpm for 15 min using a Multimix CKL mixer at room temperature to form HIPE, which was allowed to age at 40 °C in an MMM Vacucell vacuum oven for 7 days for the formation of calcium phosphate crystals. The pH of the HIPE reaction medium containing calcium and phosphate ions was determined at the initial and end of the aging period using an Orion Model 420A pH meter fitted with a Ross pH electrode at 25 °C. In order to retrieve the precipitates, ethanol (98%, Fluka) was added to demulsify the HIPE system. The demulsified HIPE was centrifuged using a Hettich centrifuge at 4500 rpm for 30 min to separate the precipitates from the medium. The washing process was repeated three times with ethanol followed by deionized water. The precipitates were then calcined at 600 °C in a Carbolite furnace for 2 h to obtain white powders. The process was repeated with 0.30 M and 0.10 M of $CaCl_2$, and 0.18 M and 0.06 M of Na_2HPO_4, respectively. Bulk calcium phosphate was prepared using conventional wet chemical processing route whereby 0.50 M $CaCl_2$ aqueous solution was titrated with 0.30 M Na_2HPO_4 aqueous solution under constant stirring, as a comparison to the HIPE-prepared calcium phosphates.

2.2. Characterization

Crystallinity of the powders was measured using a Phillips X-ray Diffractometry (XRD). The as-prepared powder was placed on a glass slide. Measurements were taken from 4° to 70° on the 2θ scale at a size step of 0.033° s^{-1}. The XRD data was processed using in-built PANalytical X'pert HighScore software to examine the peak position and its corresponding intensity data. Chemical bonding of the powders was analyzed using a Perkin-Elmer Fourier transform infrared (FTIR) spectroscopy. The powders were mixed with potassium bromate, ground homogenously and converted into pellets. The spectra (% transmittance with wave number) were recorded. The morphology of the powders was observed using a LEO 1455 Variable Pressure Scanning Electron Microscopy (VPSEM). The powders were mounted on aluminum stubs using double-sided tape and vacuum coated with gold in a Polaron SC500 sputter coater.

2.3. Cytotoxicity test

Cytotoxicity test was carried out for the evaluation of cell compatibility in direct contact with brushite crystals. HIG-82 cell line (synoviocytes) was purchased from American Type Culture Collection (ATCC, Manassas, USA) and cultured in the

Dulbecco's Modified Eagle's Medium (DMEM) supplemented with 10% fetal bovine serum, 4.5 g/l glucose, 1.0 mM sodium pyruvate, 2.0 mM L-glutamine, 50 μg/ml streptomycin and 50 μg/ml penicillin at 37 °C in a humidified atmosphere of 5% CO_2. Cells at a confluency of 80–90% were detached by typsin–EDTA (0.25%) and centrifuged at 110 × *g* at 4 °C for 5 min. The concentration was then adjusted to 8×10^5 cells/ml and cell viability was >95% as determined by the trypan blue dye exclusion.

Prior to cell seeding, the calcium phosphate powders were pelletized, ball milled, sintered at 1100 °C, and sterilized by washing three times with ethanol and gamma-irradiated at 40 kGy. The sintered samples were examined with XRD to ensure that there was no change in the crystalline phases. Cell suspension (100 μl) was dispensed into wells of 96-well culture plates (8×10^4 cells/well) containing the crystals and incubated for 5 days at 37 °C of 5% CO_2. MTT (3-(4,5-dimethylthiazol-2-yl)-2,5-diphenyl tetrasodium bromide) assay and SEM examination were conducted at days 1, 3 and 5. The culture medium was replaced every alternate day with care to ensure minimum disruption of cells.

The MTT assay was used to measure the viability of cells with the brushite crystals. The cytotoxicity of the crystals towards cultured cells was determined by reduction of MTT reagent to dark blue formazane dye by mitochondrial dehydrogenases of living cells. After 1, 3 and 5 days, 20 μl MTT (5 mg/ml) was added to each well and incubated at 37 °C with 5% CO_2 and absorbance was measured after 4 h of contact at 570 nm using a SpectraMax Plus microplate reader. The results were expressed as cell viability in percentage of three replicates ($n = 3$). Statistical analysis was performed using one-way analysis of variance (ANOVA) following Dunnett's test post hoc for multi-group comparison test. Statistical significance of differences between groups was accepted at p value <0.05.

Prior to examination under a Phillips XL30 Environmental Scanning Electron Microscopy (ESEM), the seeded samples were put into separate vials and fixed in 4% glutaraldehyde for 1–2 h at 4 °C. The samples were washed with 0.1 M sodium cacodylate buffer for three changes of 10 min each and post fixed in 1.0% osmium tetroxide for 2 h at 40 °C. The samples were washed again with 0.1 M sodium cacodylate buffer for three changes of 10 min each and dehydrated with a series of acetone; 35% 10 min, 50% 10 min, 75% 10 min, 95% 10 min and 100% 15 min (three changes). Critical point drying was performed with a Baltec critical point dryer for 30 min before mounting the samples onto stubs and gold coating them with a Baltec sputter coater.

3. Results and discussion

Fig. 1 shows that the XRD patterns of the bulk and the as-prepared crystals portray almost similar diffraction profiles. The diffraction peaks of the powders were indexed to brushite crystal structure (JCPDS file no. 2-0085) with trace amount of hydroxyapatite (JCPDS file no. 1-89-4405). No characteristic peaks of other calcium phosphate phases and impurities were detected. The intensity of the diffraction peaks indicates that the samples were well-crystallized. According to our XRD results, the main calcium phosphate phase formed is brushite. This is contrary to the literature that the main calcium phosphate phase at the Ca/P concentration ratio of 1.67 is hydroxyapatite (HA). Based on the explanation by Singh et al. [38], 5 units of $CaCl_2{\cdot}2H_2O$ reacting with 3 units of Na_2HPO_4 are not sufficiently alkaline for producing pure HA. Eq. (2) shows that the formation of HA will form $4H^+$ ions:

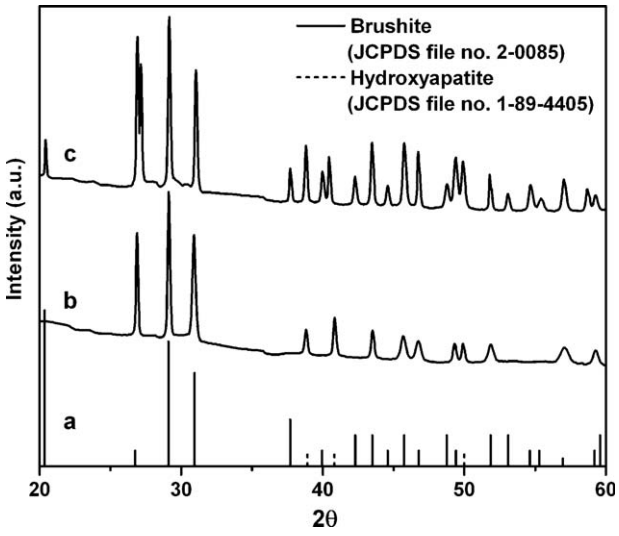

Fig. 1. XRD patterns of (a) JCPDS standards of brushite and hydroxyapatite, (b) bulk brushite and (c) brushite crystals prepared with 0.50 M calcium ion and 0.30 M phosphate ion.

$$5CaCl_2{\cdot}2H_2O + 3Na_2HPO_4 \rightarrow Ca_5(PO_4)_3OH(s) + 4H^+ + 10Cl^- + 6Na^+ + 9H_2O \quad (2)$$

About $3H^+$ ions will be released even if only calcium-deficient hydroxyapatite is formed. A release of 3–4 H^+ ions per unit of HA formation causes a significant decrease in solution pH. Brushite becomes more stable than HA when pH is <6.5 [39–42]. Our work was in agreement with the explanation above as the pH of the HIPE reaction medium containing calcium and phosphate ions at the initial aging period was ~4.5 and the final pH was ~3.8. That is why brushite is the major phase in all the samples. Brushite formation is also contributed by the low reaction temperature of 40 °C [43]. It was found that the relative intensity of diffraction peak at $2\theta = 26.8^\circ$ for the HIPE-prepared brushite is higher than the standard because of their preferential growth along a certain crystal plane due to constraint within the continuous phase of HIPE [44]. The result is consistent with the SEM observation which shows elongation of the crystals.

Fig. 2 shows the FTIR spectra of the HIPE-prepared brushite crystals, which is based on our previous work [45]. The spectrum is free from alkyl group, signifying the absence of residual organic materials. The broad band at 3000–3800 cm^{-1} is caused by stretching and bending of residual-free water. Additional band at 1600 cm^{-1} is attributed to bending mode of O–H group due to absorbed water. The weak band at 2900 cm^{-1} is assigned to O–H stretching of brushite [5]. The spectrum

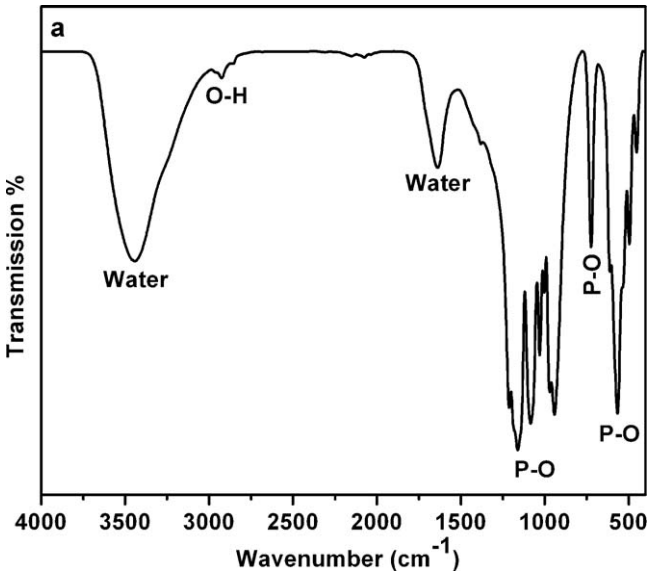

Fig. 2. FTIR spectrum of brushite crystals prepared with 0.50 M and 0.30 M of $CaCl_2$, and Na_2HPO_4.

exhibits easily distinguishable bands attributed to PO_4^{3-}. The bands in the range of 430–520 cm^{-1}, 520–630 cm^{-1} and 720 cm^{-1} are assigned to υ_2 O–P–O bending mode, υ_4 O–P–O bending mode and phosphate group bending mode, respectively [13,47]. The bands at 900–990 cm^{-1} and 990–1250 cm^{-1} are assigned to υ_1 symmetric P–O stretching mode and υ_3 antisymmetric P–O stretching mode, respectively [24]. The

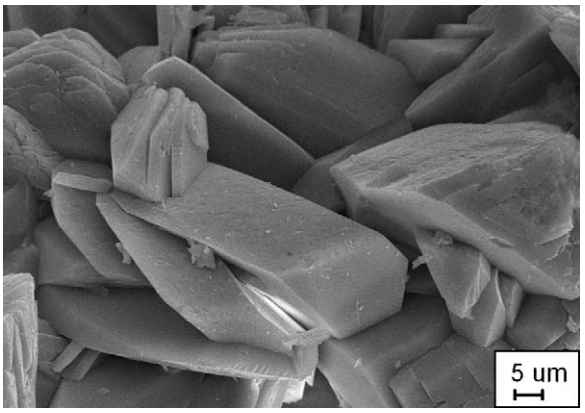

Fig. 3. SEM image of bulk brushite.

PO_4^{3-} bands extensive split at 1125 cm^{-1} suggests high crystallinity of the brushite crystals which is consistent with the XRD result.

Brushite crystals prepared by conventional processing route was bulky in size due to the absence of a reaction medium during preparation as shown in Fig. 3. The morphology consists of merged large plates forming irregular chunky material with dimension of more than 10 μm. In contrast, brushite crystals obtained through the HIPE approach had smaller dimensions and unique morphologies as exhibited by the SEM micrographs. The differences come from the reaction media employed and indicated that the emulsion shows a template effect on the crystal growth to some extent [46]. The

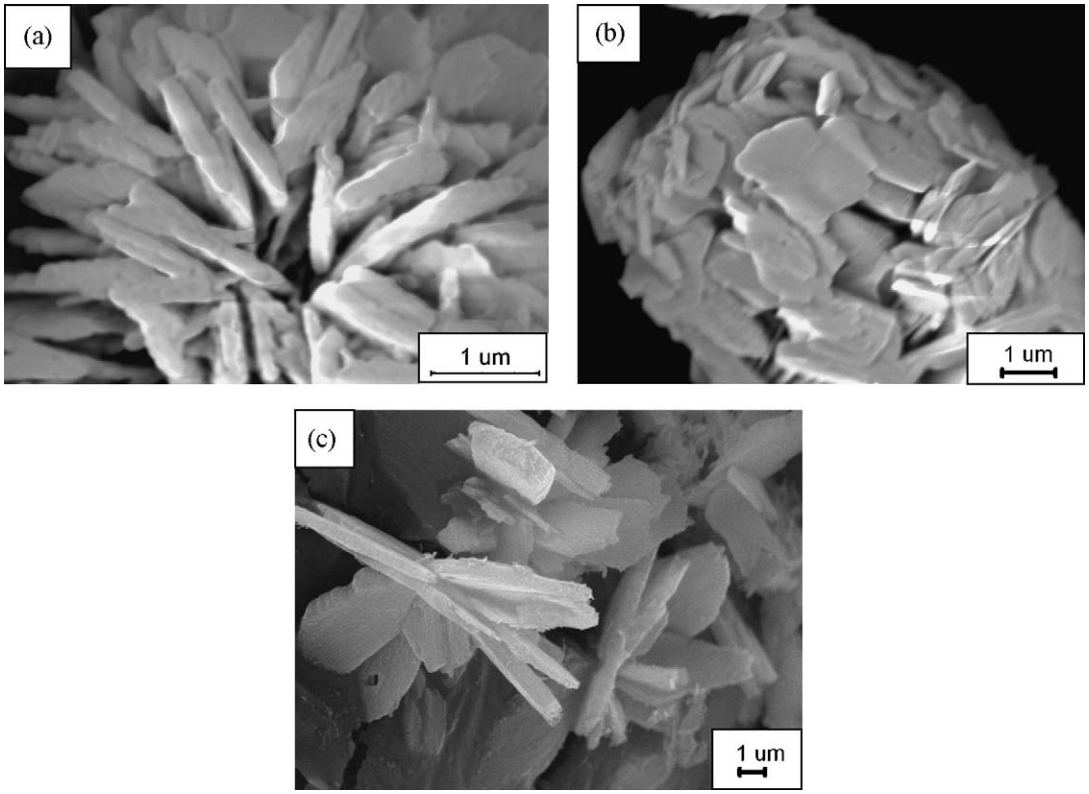

Fig. 4. SEM images of brushite crystals prepared with (a) 0.50 M and 0.30 M, (b) 0.30 M and 0.18 M, and (c) 0.10 M and 0.06 M of $CaCl_2$, and Na_2HPO_4, respectively.

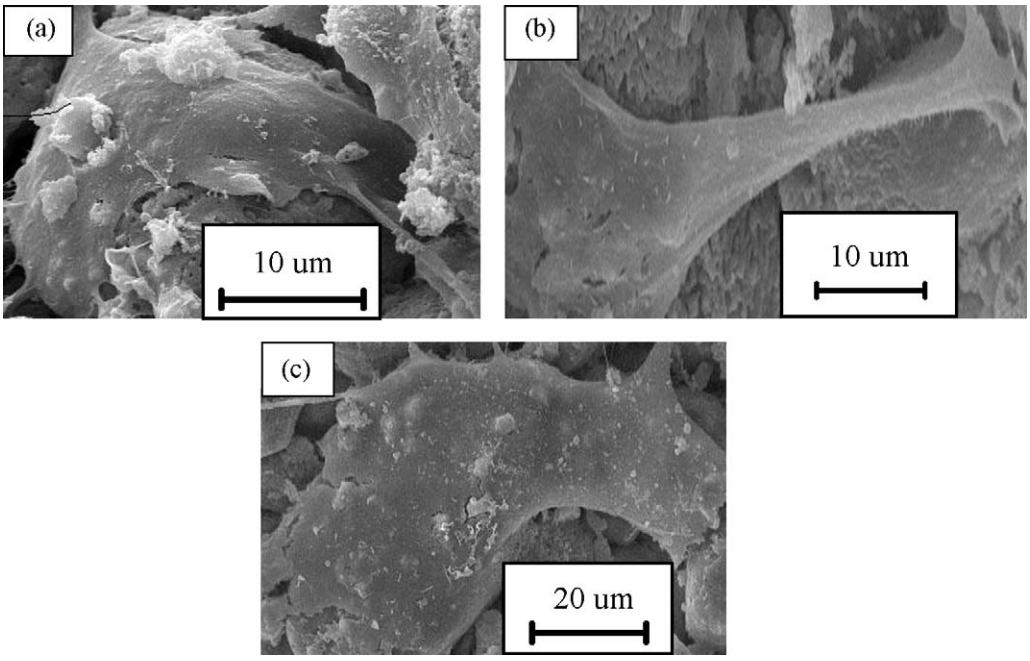

Fig. 5. The morphology of the synoviocytes adhering and spreading on the brushite crystals on the (a) 1st day, (b) 3rd day and (c) 5th day.

hydrophile–lipophile balance (HLB) of Brij 35 is more than 10 based on calculation using the Griffin equation [47]. Hence, it is a water soluble surfactant, in which it is able to form oil-in-water emulsion. The hydrophobic lauryl alcohol tails anchor on the surface of the discontinuous oil droplets thus, covering these droplets to resemble the continuous aqueous phase. On the other hand, the hydrophilic polyoxyethylene head groups project towards the continuous aqueous phase. The self-assembly of the surfactant molecules forms O/W HIPE, where the reaction between calcium and phosphate ions takes place within the geometry of the continuous aqueous phase.

The morphology of brushite crystals is very much dependent on the precursor concentration. The fast rate of nucleation and crystal growth as a result of the high precursor concentration [48] led to better defined flower-like structures. Fig. 4a shows the SEM image of brushite crystal prepared with 0.50 M and 0.30 M of calcium and phosphate ions, respectively. The crystal takes after the shape of a carnation composing of similar petal-like flakes growing radially from the centre. Fig. 4b consists of bud-like cluster of flakes connecting to one another, which was prepared with 0.30 M and 0.18 M of calcium and phosphate ions, respectively. The sparse flake arrangement shown in Fig. 4c, which was prepared with 0.10 M and 0.06 M of calcium and phosphate ions, respectively, gives rise to lotus-like morphology.

Fig. 5 illustrates the morphology of the synoviocytes adhering to the brushite crystals at different incubation periods for 5 days. It is obvious that the synoviocytes adhered and spread on the ceramic surface, which resulted in flattened morphology. The adhered cells presented a close contact with the surface of the crystals, which was the characteristic morphology on the three different incubation days. Interestingly, the synoviocytes maintained their robustness with the increase of the length-to-diameter ratio of the cell by almost twofold on the 5th day (Fig. 5c), which is in agreement with Tomasek and Hay [49], indicative of the cells' strong adherence on the brushite crystals' surface. The brushite crystals neither caused cytotoxicity nor significant difference in the proliferation rate of the cells on the three different incubation days as shown in Fig. 6. The cell morphology and cell viability reflect the promising cytocompatibility properties of the crystals. Therefore, the brushite crystals provided a cell-favourable environment for the synovium tissue regeneration, in which

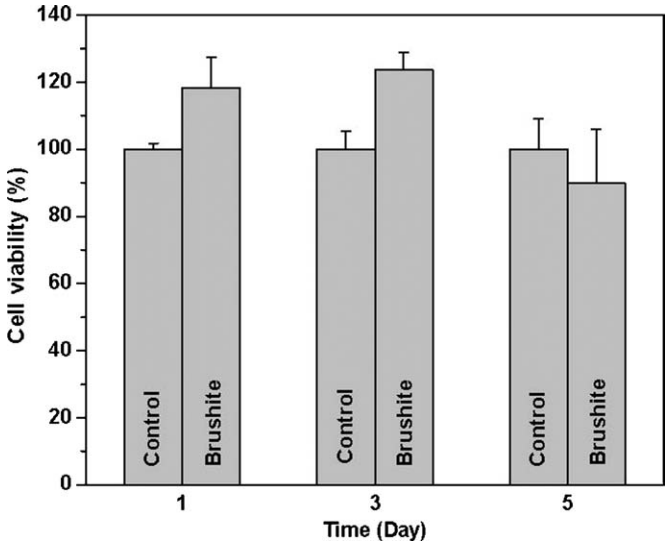

Fig. 6. Effects of the brushite crystals on the viability of synoviocytes. All values represent mean of triplicates of the experiment ($n = 3$). Statistical analysis using ANOVA (Dunnett's test post hoc) was performed and there is no significant difference of the group treated with brushite crystals at day 1, day 3 and day 5 when compared with the control group (p value >0.05).

brushite is suitable to be used as a synthetic bone replacement material.

The formation of intimate bond between the cells surrounding the implant and the implant material is important as it obligates cell adherence. Cells fail to proliferate, grow and differentiate if they are denied a substrate on which they can adhere [50]. This anchorage dependence is a prerequisite for bone formation in vitro [51] and in vivo [52]. Therefore, osteoconduction is closely associated with the phenomenological behaviour of cells to anchor, attach, adhere and spread, and the process of bone formation requires a surface that allows this cell behaviour [53]. The as-prepared brushite crystals clearly favour cell proliferation.

4. Conclusion

Flower-like brushite crystals were successfully synthesized using O/W HIPE for the first time. The crystals' morphology could be controlled by varying the precursor concentration. Higher precursor concentration yielded brushite crystals with well defined morphology. The cell experiments showed that the brushite crystals supported growth and adhesion of synoviocytes thus, demonstrating good biocompatibility of the crystals. The brushite crystals had proven to be a suitable bioceramic coating for non-biocompatible bone implants as exhibited by their ability to sustain the cells.

Acknowledgement

The author (H.N. Lim) would like to thank Universiti Putra Malaysia for the award of Graduate Research Fellowship.

References

[1] Y. Wu, S. Bose, Nanocrystalline hydroxyapatite: micelle templated synthesis and characterization, Langmuir 21 (2005) 3232–3234.
[2] C. Ritzoulis, N. Scoutaris, K. Papademetriou, S. Stavroulias, C. Panayiotou, Milk protein-based emulsion gels for bone tissue engineering, Food Hydrocolloids 19 (2005) 575–581.
[3] K. Soballe, Hydroxyapatite ceramic coating for bone implant fixation. Mechanical and histological studies in dogs, Acta Orthopaedica Scandinavica Supplementum 255 (1993) 1–58.
[4] K. Ishizaki, S. Komarneni, M. Nanko, Porous Materials: Process Technology and Applications, Kluwer Academic, London, 1998.
[5] O. Lyckfeldt, J.M.F. Ferreira, Processing of porous ceramics by ''starch consolidation'', Journal of European Ceramic Society 18 (1998) 131–140.
[6] T. Takaoka, M. Okumura, H. Ohgushi, K. Inoue, Y. Takakura, S. Tamai, Histological and biochemical evaluation of osteogenic response in porous hydroxyapatite-coated alumina ceramics, Biomaterials 17 (1996) 1499–1505.
[7] M. Taniguchi, H. Takeyama, I. Mizuno, N. Shinagawa, J. Yura, N. Yoshikawa, H. Aoki, The clinical application of intravenous catheter with percutaneous device made of sintered hydroxyapatite, Japanese Journal of Artificial Organs 20 (1991) 460–464.
[8] J.C. Le Huec, D. Clement, B. Brouillaud, N. Barthe, B. Dupuy, B. Foliguet, B. Basse-Cathalinat, Evolution of the local calcium content around irradiated-tricalcium phosphate ceramic implants: in vivo study in the rabbit, Biomaterials 19 (1998) 733–738.
[9] F. Barrere, A. Lebugle, C.A. Van Blitterswijk, K. De Groot, P. Layrolle, C. Rey, Calcium phosphate interactions with titanium oxide and alumina substrates: an XPS study, Journal of Materials Science: Materials in Medicine 14 (2003) 419–425.
[10] M. Bohner, Calcium orthophosphates in medicine: from ceramics to calcium phosphate cements, Injury 31 (2000) 37–47.
[11] A.A. Mirtchi, J. Lemaitre, N. Terao, Calcium phosphate cements: study of the beta-tricalcium phosphate–monocalcium phosphate system, Biomaterials (1989) 475–480.
[12] L.M. Grover, J.C. Knowles, G.J.P. Fleming, J.E. Barralet, In vitro dissolution of brushite cement, Biomaterials 24 (2003) 4133–4141.
[13] G. Penel, N. Leroy, P. Van Landuyt, B. Flautre, P. Hardouin, J. Lemaitre, G. Leroy, Raman microspectrometry studies of brushite cement: in vivo evaluation in a sheep model, Bone 25 (1999) 81S–84S.
[14] P. Fraysinnet, L. Gineste, P. Conte, J. Fages, N. Rouquet, Short term implantation effects of a DCPD based calcium phosphate cement, Biomaterials 19 (1998) 971–977.
[15] M. Vallet-Regí, C.V. Ragel, A.J. Salinas, Glasses with medical applications, European Journal of Inorganic Chemistry (2003) 1029–1042.
[16] L. Vaz, A.B. Lopes, M. Almeida, Porosity control of hydroxyapatite implants, Journal of Materials Science: Materials in Medicine 10 (1999) 239–242.
[17] X. Miao, Y. Hu, J. Liu, A.P. Wong, Porous calcium phosphate ceramics prepared by coating polyurethane foams with calcium phosphate cements, Materials Letters 58 (2004) 397–402.
[18] C. Solans, J. Esquena, N. Azemar, Highly concentrated (gel) emulsions, versatile reaction media, Current Opinion in Colloid Interface Science 8 (2003) 156–163.
[19] R. Pal, Rheology of high internal phase ratio emulsions, Food Hydrocolloids 20 (2006) 997–1005.
[20] T. Iwanaga, M. Shikichi, H. Kitamura, H. Yanase, K. Nozawa-Inoue, Morphology and functional roles of synoviocytes in the joint, Archives of Histology and Cytology 63 (2000) 17–31.
[21] M. Bouchgua, K. Alexander, M.A. d'Anjou, C.A. Girard, E.N. Carmel, G. Beauchamp, H. Richard, S. Laverty, Use of routine clinical multimodality imaging in a rabbit model of osteoarthritis. Part I, Osteoarthritis and Cartilage 17 (2009) 188–196.
[22] M. Bouchgua, K. Alexander, E.N. Carmel, M.A. d'Anjou, G. Beauchamp, H. Richard, S. Laverty, Use of routine clinical multimodality imaging in a rabbit model of osteoarthritis. Part II. Bone mineral density assessment, Osteoarthritis and Cartilage 17 (2009) 197–204.
[23] H.I. Georgescu, D. Mendelow, C.H. Evans, HIG-82: an established cell line from rabbit periarticular soft tissue, which retains the ''activatable'' phenotype, In Vitro Cellular and Developmental Biology 24 (1998) 1015–1022.
[24] C.E. Brinckerhoff, R.M. McMillan, J.V. Fahey, E.D.J. Harris, Collagenase production by synovial fibroblasts treated with phorbol myristate acetate, Arthritis and Rheumatism 22 (1979) 1109–1116.
[25] J.M. Dayer, S.M. Krane, R.G.G. Russell, D.R. Robinson, Production of collagenase and prostaglandins by isolated adherent rheumatoid synovial cells, Proceedings of the National Academy of Sciences of the United States of America 73 (1976) 945–949.
[26] F.H. Ghadially, S. Rov, Ultrastructure of Synovial Joints in Health and Disease, Butterworth, London, 1969.
[27] B.A. Ashton, I.K. Ashton, M.J. Marshall, R.C. Butler, Localization of vitronectin receptor immunoreactivity and tartrate resistant acid phosphatase activity in synovium from patients with inflammatory and degenerative arthritis, Annals of the Rheumatic Diseases 52 (1993) 133–137.
[28] Y. Fujikawa, A. Sabokbar, S. Neale, N.A. Athanasou, Human osteoclast formation and bone resorption by monocytes and synovial macrophages in rheumatoid arthritis, Annals of the Rheumatic Diseases 55 (1993) 816–822.
[29] J.S. Chang, J.M. Quinn, A. Demaziere, C.J. Bulstrode, M.J. Francis, R.B. Duthie, N.A. Athanasou, Bone resorption by cells isolated from rheumatoid synovium, Annals of the Rheumatic Diseases 51 (1992) 1223–1229.
[30] M. Chabaud, J.M. Durand, N. Buchs, Human interleukin-17: a T cell-derived proinflammatory cytokine produced by the rheumatoid synovium, Arthritis and Rheumatism 42 (1999) 963–970.
[31] S. Kotake, N. Udagawa, N. Takahashi, K. Matsuzaki, K. Itoh, S. Ishiyama, S. Saito, K. Inoue, N. Kamatani, M.T. Gillespie, T.J. Martin, T. Suda, IL-17 in synovial fluids from patients with rheumatoid arthritis is a potent

stimulator of oteoclastogenesis, The Journal of Clinical Investigation 103 (1999) 1345–1352.
[32] J.L. Funk, L.A. Cordaro, H. Wei, J.B. Benjamin, D.E. Yocum, Synovium as a source of increased amino-terminal parathyroid hormone-related protein expression in rheumatoid arthritis. A possible role for locally produced parathyroid hormone-related protein in the pathogenesis of rheumatoid arthritis, The Journal of Clinical Investigation 101 (1998) 1362–1371.
[33] E. Romas, T.J. Martin, Cytokines in the pathogenesis of osteoporosis, Osteoporosis International 7 (1997) 547–553.
[34] C.Q. Chu, M. Field, S. Allard, E. Abney, M. Feldmann, R.N. Maini, Detection of cytokines at the cartilage/pannus junction in patients with rheumatoid arthritis; implications for the role of cytokines in cartilage destruction and repair, Rheumatology 32 (1992) 653–661.
[35] B.W. Deleuran, C.Q. Chu, M. Field, F.M. Brennan, P. Katsikis, M. Feldmann, R.N. Maini, Localization of interleukin-1a, type 1 interleukin-1 receptor and interleukin-1 receptor antagonist in the synovial membrane and cartilage/pannus junction in rheumatoid arthritis, Rheumatology 31 (1992) 801–809.
[36] C.Q. Chu, M. Field, M. Feldman, R.N. Maini, Localization of tumour necrosis factor-a in synovial tissue and at the cartilage–pannus junction in patients with rheumatoid arthritis, Arthritis and Rheumatism 34 (1991) 1125–1132.
[37] B. Niraula, C.K. Tan, K.C. Tham, M. Misran, Rheology properties of glycopyranoside stabilized oil–water emulsions: effect of alkyl chain length and bulk concentration of the surfactant, Colloids and Surfaces A: Physicochemical and Engineering Aspects 251 (2004) 117–132.
[38] S. Singh, P. Bhardwaj, V. Singh, S. Aggarwal, U.K. Mandal, Synthesis of nanocrytalline calcium phosphate in microemulsion-effect of nature of surfactants, Journal of Colloid and Interface Science 319 (2008) 322–329.
[39] A. Ferreira, C. Oliveira, F. Rocha, The different phases in the precipitation of dicalcium phosphate dihydrate, Journal of Crystal Growth 252 (2003) 599–611.
[40] J.C. Elliott, Structure and Chemistry of the Apatites and Other Calcium Orthophosphates, Elsevier, Amsterdam, 1994.
[41] F. Abbona, H.E.L. Madsen, R. Boistelle, The initial phases of calcium and magnesium phosphates precipitated from solutions of high to medium concentrations, Journal of Crystal Growth 74 (1986) 581–590.
[42] H.E.L. Madsen, F. Christensson, Precipitation of calcium phosphate at 40 °C from neutral solution, Journal of Crystal Growth 114 (1991) 613–618.
[43] P.N. Kumta, C. Sfeir, D.H. Lee, D. Olton, D.W. Choi, Nanostructured calcium phosphates for biomedical applications: novel synthesis and characterization, Acta Biomaterialia 1 (2005) 65–83.
[44] N.M. Huang, S. Radiman, H.N. Lim, S.K. Yeong, P.S. Khiew, W.S. Chiu, S.N. Kong, G.H.M. Saeed, Synthesis and characterization of ultra small PbS nanorods in sucrose ester microemulsion, Materials Letters 63 (2009) 500–503.
[45] H.N. Lim, A. Kassim, N.M. Huang, R. Hashim, S. Radiman, P.S. Khiew, W.S. Chiu, Fabrication and characterization of 1D brushite nanomaterials via sucrose ester reverse microemulsion, Ceramics International 35 (2009) 2891–2897.
[46] K. Sonoda, T. Furuzono, D. Walsh, K. Sato, J. Tanaka, Influence of emulsion on crystal growth of hydroxyapatite, Solid State Ionics 151 (2002) 321–327.
[47] W.C. Griffin, Classification of surface-active agents by "HLB", Journal of the Society of Cosmetic Chemist 1 (1949) 311–326.
[48] M.P. Pileni, Reverse micelles used as templates: a new understanding in the nanocrystal growth of silver and copper nanocrystals by using hydrazine as reducing agent, Journal of Experimental Nanoscience 1 (2006) 13–27.
[49] J.J. Tomasek, E.D. Hay, Analysis of the role of microfilaments and microtubules in acquisition of bipolarity and elongation of fibroblasts in hydrated collagen gels, The Journal of Cell Biology 99 (1984) 536–549.
[50] M. Stoker, C. O'Neil, Anchorage and growth regulation in normal and virus transformed cells, International Journal of Cancer 3 (1968) 683–693.
[51] R.E. Weiss, C. Itatani, The role of fibronectin and substrate size in attachment of rat bone marrow cells, SEMicroscopy (1981) 183–188.
[52] J.J. Stutzmann, A.G. Petrovic, Bone cell histogenesis: the skeletoblast as a stem-cell for preosteoblasts and secondary-type prechondroblasts, in: A.D. Dixon, B.G. Sarnat (Eds.), Factors and Mechanisms Influencing Bone Growth, Alan R Liss, New York, 1982, pp. 29–43.
[53] E. Tsiridis, N. Gurav, G. Bailey, R. Sambrook, L. Di Silvo, A novel ex vivo culture system for studying bone repair, Injury 37 (2006) 10–17.